Regrowth of oxide-embedded amorphous silicon studied with molecular dynamics

E. Lampin, Christophe Krzeminski

Regrowth of oxide-embedded amorphous silicon studied with molecular dynamics

Cite as: J. Appl. Phys. **109**, 123509 (2011); https://doi.org/10.1063/1.3596815
Submitted: 18 March 2011 • Accepted: 30 April 2011 • Published Online: 20 June 2011

E. Lampin and C. Krzeminski

Regrowth of oxide-embedded amorphous silicon studied with molecular dynamics

E. Lampin[a] and C. Krzeminski
IEMN, Avenue Poincaré, 59652 Villeneuve d'Ascq Cedex, France

(Received 18 March 2011; accepted 30 April 2011; published online 20 June 2011)

Classical molecular dynamics simulations are applied to the study of amorphous silicon regrowth in a nanodevice. A simplified atomistic amorphous nanostructure presenting the main features of a FinFET device is designed. A thermal treatment is used to simulate the annealing of the atomic model. The structure after annealing is very close to what observed experimentally, with perfect crystal near the silicon seed, an intermediate crystalline layer presenting [111] twins, and an upper terminal region of polysilicon. The comparison with 2D system suggests surface proximity effects that impact the probability to form grains and twins. As a consequence, it seems like the solid phase epitaxy was arrested in the nanostructure. © *2011 American Institute of Physics*.
[doi:10.1063/1.3596815]

I. INTRODUCTION

Heavy-ion bombardment of silicon at high dose is a widely used method to form ultrashallow source-drain junctions in advanced electronic circuits. This is achieved by amorphization of the surface layer, thereby limiting the penetration of dopants in the bulk. During post-annealing, a solid phase epitaxy (SPE) is initiated at the interface between crystalline (cSi) and amorphous (aSi) silicon, and the interface progresses toward the surface until complete regrowth. This phenomenon is well studied from both the experimental[1] and theoretical[2–4] point of view. Nevertheless, in nanostructures as encountered in fin field-effect transistors[5] (FinFETs), the regrowth of amorphous silicon is not as straightforward. In fact, some observations have evidenced defective regions and polysilicon, in annealing conditions where the regrowth of the amorphous would have been perfect in 2D structures. It has been proposed that SPE could be retarded in the nanostructure, so that crystallites could nucleate homogeneously far from the seed, and form polysilicon (polySi) by random nucleation and growth (RNG). We have carried out atomistic simulations to investigate the role of confinement on the regrowth of aSi, and in particular on the SPE velocity.

The simulations are performed using the classical molecular dynamics method using Tersoff interatomic potential.[6] This technique is adapted to the study of SPE at the atomic scale.[2,3,7] It has also been used to study homogeneous nucleation,[8] nonetheless without reaching the regime of growth of the nuclei that leads to polySi. In Sec. II, we describe the atomic model used for the calculations. The simulated regrowth of this system is presented in Sec. III. We show that simulation correctly reproduces the three zones observed in experiments, i. e., perfect cSi, defective cSi and polySi. The results of the calculations are discussed and compared to 2D calculations in Sec. IV before concluding.

[a]Electronic mail: evelyne.lampin@isen.iemn.univ-lille1.fr.

II. ATOMISTIC SYSTEM

A schematic structure of the experimental device that we study by computer simulation is given in Fig. 1. The left view presents the silicon fin embedded in SiO_2 (in black on the figure). The structure has been ion implanted by the top. Under the gate, the oxide is thicker and the fin is not amorphized (cSi in white), while under the source and drain the fin is nearly fully amorphized (aSi in gray). A thin residual crystalline region (in white) is left at the bottom of the fin. In the middle picture of Fig. 1, a cross view of the fin in the source-drain after implantation is schematized. The restricted thickness of cSi and the presence of surfaces with SiO_2 all around the fin are highlighted. In the right view, the scheme shows the fin after rapid thermal annealing (RTA) at 1050 °C, i.e., the typical conditions leading to regrowth of aSi in layer. The bottom part is crystalline, the upper part is polycrystalline, and an intermediate region presents twin defects in {111} planes. The dimensions of the fin section are 60 nm high and around 15–20 nm wide.

In order to model the fin, we have to: (i) build an atomistic model of the crystalline fin surrounded by the silicon oxide and (ii) simulate the destruction of the crystalline structure by ion implantation. These two steps are already challenging, as we will discuss hereafter. To circumvent such difficulties, we have instead designed the atomistic structure presented in Fig. 2. The core of the fin (black atoms represented by balls connected by sticks) is amorphous, at the exception of a crystalline seed of a few atomic layers at the bottom. The fin is oriented along [001]. The amorphous layer was not obtained by simulating the ion implantation. Indeed, the description of ion implantation by molecular dynamics is not realistic since a good quality of aSi requires the simulation of a large number of ion implantations, and for each of this events the relaxation of the full atomic box in opposition to the binary collision approximation method.[9] Instead, more artificial methods are commonly used to create a computer model of the aSi cluster, either using a bond switching algorithm[10] or the method of melting-quenching.[11]

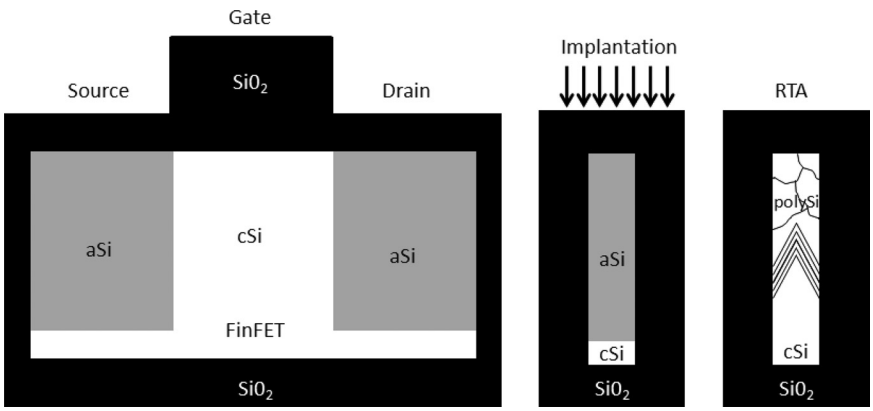

FIG. 1. Schematics of the FinFET structure of Ref. 5. (a) plane view after implantation. (b) cross view after implantation. (c) cross view after annealing.

In previous works, we already used both methods to study the amorphous silicon regrowth, and show that the velocity of regrowth obtained in the two cases are similar.[12] In the present work, we have scaled the velocities to simulate melting at 3500 K followed by quenching at 10 K/ps of the main part of the system. A few atomic planes at the bottom are frozen. Periodic boundary conditions are applied along [010] and [001]. The (100) surface is let free to allow for thermal expansion and compression. The quality of the aSi part was checked by looking at the radial and angular distribution functions (Fig. 3). A distinct first peak is followed by a drop to zero in the radial distribution. An angular spreading of 15° is obtained around the crystalline angle of 109.5°. These features demonstrate a good quality of the aSi simulated system. A full description of the outer layers of SiO_2 adds the complication of the choice of Si-O parametrization[13–16] that will result in a realistic Si/SiO_2 interface. Instead, we proposed a simplification, based on a shell of frozen silicon atoms in an amorphous arrangement. These will provide the core atoms with the two effects of: (1) an interface with a material not promoting a SPE, since it is not crystalline, and (2) a confinement in two directions. To this end, after creating the amorphous on crystalline stack, a 7 Å-thick- and [001]-parallel shell of atoms was frozen in order to mimic the oxide of the real device (atoms represented by red dots in Fig. 2). The thickness of 7 Å was chosen after several attempts, in order to maintain the confinement of the black atoms in the inner region of the fin. The width of the fin (core + shell) is equal to 4.6 nm and its height is 13.8 nm. The aspect ratio of the experimental structure is preserved, although the actual size of the simulated structure is four times smaller in both directions, in order to permit reasonable computer times. The depth of the structure is 4.3 nm, for a total number of atoms equal to 12800. Periodic boundary conditions are applied in the [001] direction, so that we simulate a fin of infinite depth.

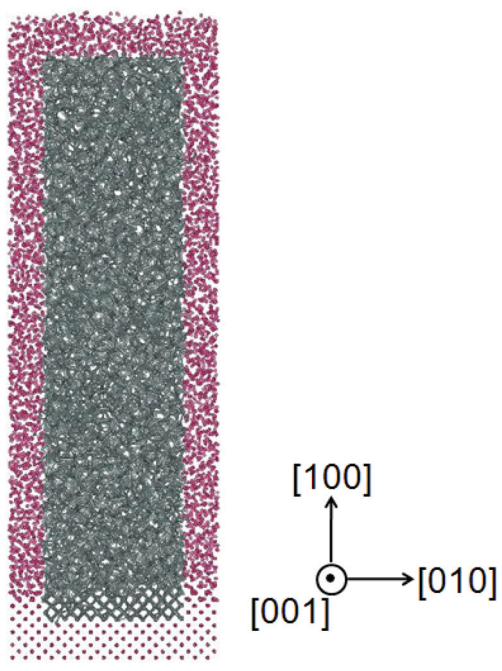

FIG. 2. (Color online) Atomistic model build to mimic the oxide embedded fin shown in Fig. 1.

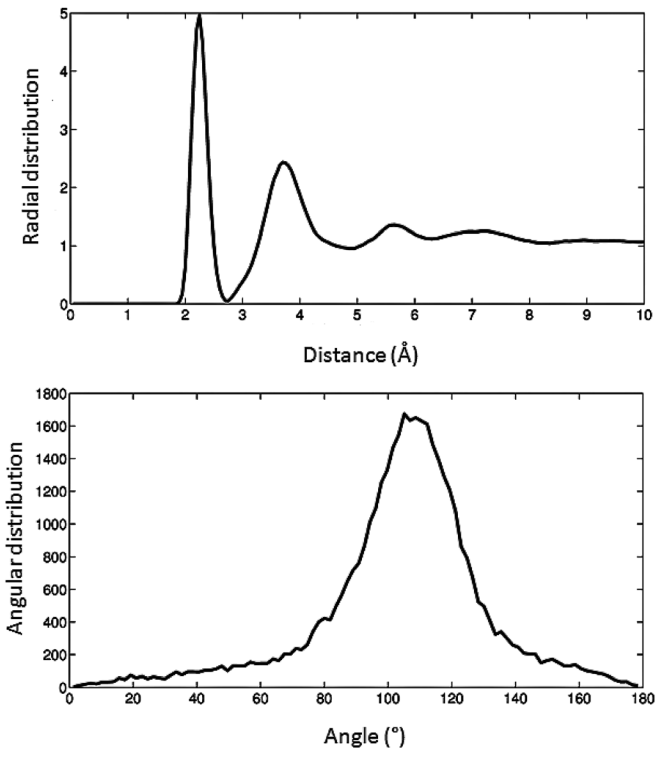

FIG. 3. Radial (a) and angular (b) distribution of the aSi cluster obtained by melting- quenching.

III. ANNEALING

The annealing of the model nanostructure was simulated by molecular dynamics using the same interatomic potential since Tersoff's description is suitable to describe the regrowth of amorphous silicon.[7] Indeed, this potential preserves the amorphous characteristics of the radial and angular distribution of the disordered part upon annealing. Moreover, the regrowth velocity extrapolates well to experimental values at low temperatures.[17] Nevertheless, it also entails a strong overestimation of the melting temperature (2500 K instead of 1700 K). This weakness of the potential is the key for the observation of SPE using molecular dynamics, since the phenomenon begins to be fast enough for the technique at $\approx$ 1500 K. If the melting temperature was not overestimated, the temperature range before melting would have been strongly reduced. In the present study, we have chosen a temperature of 1700 K to keep in the SPE regime far from melting. In the following, we present the results obtained upon annealing of the atomic structure. After equilibration at 1700 K by velocity scaling, a Nosé-Hoover[18,19] thermostat is applied. In order to completely visualize the atomic structure, and possible grains with variable orientations, we present three views of the atomic structures (see Fig. 4). View 1 is perpendicular to the Section, i.e., along, [001] view 2 is a side view, along [010] and view 3 is along the direction, [011] a direction suited for the visualization of the twins. The three views are given after 30 ns (Fig. 5), 60 ns (Fig. 6), 90 ns (Fig. 7) and 120 ns (Fig. 8). For a better visualization, only crystal-like atoms are drawn, following the criterium $A_i < 0.2$ for each atom i where:

$$A_i = \sum \left(\cos\theta + \frac{1}{3} \right)^2 \tag{1}$$

where the sum is on the angles θ formed with the pairs of neighbors of i. In a crystal at 0 K, A is equal to 0. A small variation from 0 is allowed to account for thermal vibrations. The value of 0.2 was adjusted to get an optimal contrast in the figures. From Figs. 5–8, the number of crystal-like atoms increases as expected.

After 30 ns annealing, Fig. 5 evidences that SPE has begun and approximately a quarter of the total height is crystallized. After 60 ns, SPE has progressed and a first twin is highlighted in the view 3 of Fig. 6. The presence of this twin hides the crystallinity of the zone in the view 1. Two grains of $\approx$ 2 nm of diameter have also appeared, and they are especially observable in the view 2. After 90 ns, the twin has propagated with SPE and a second one has formed. The blurred zone in the view 1 expands upward. The grains are growing and reach diameters of $\approx$ 3 nm. After 120 ns, the density of crystal-like atoms is the highest. The two grains nearly fill the upper third. Notably, neither the SPE region nor the twin, have really progressed compared to Fig. 7. This means that a region crystallized by RNG cannot be recovered by SPE.

We have checked that the annealing of the system was completed by looking at the potential energy (Fig. 9). The energy decreases until 150 ns. The final atomic structure is

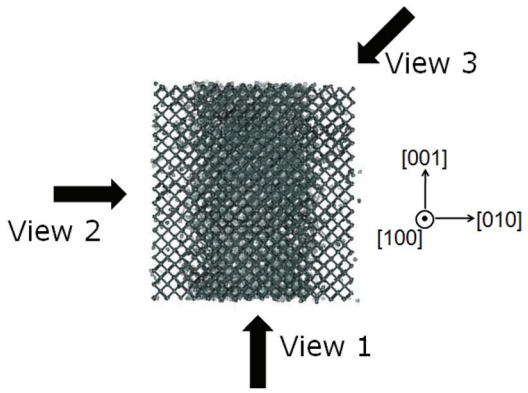

FIG. 4. (Color online) Definition of the views 1, 2 and 3. Top view of the fin.

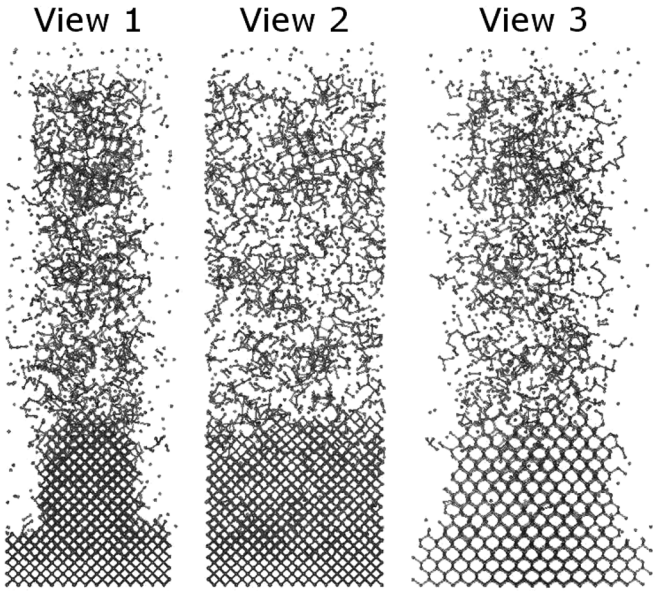

FIG. 5. Three views of the fin atomic model after 30 ns annealing. Only crystal-like atoms are represented.

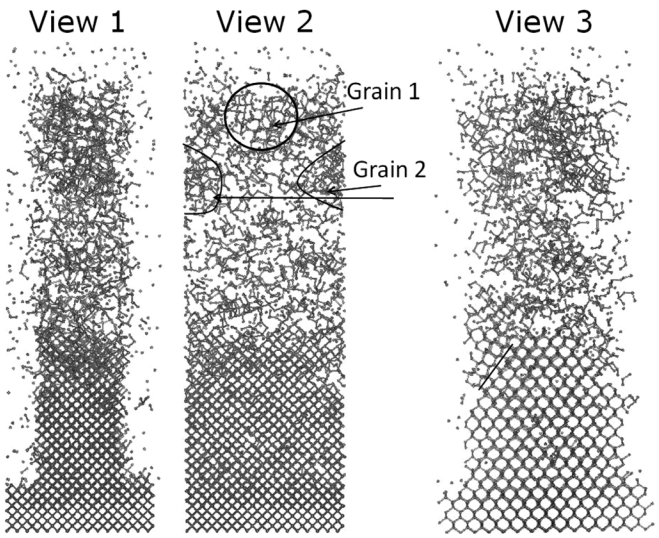

FIG. 6. Three views of the fin atomic model after 60 ns annealing. Only crystal-like atoms are represented.

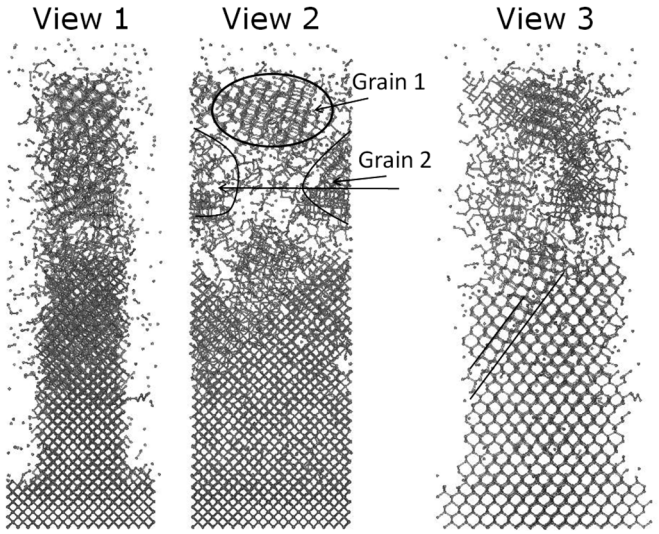

FIG. 7. Three views of the fin atomic model after 90 ns annealing. Only crystal-like atoms are represented.

presented in Fig. 10. The system is formed of a bottom third of cSi, a middle third of cSi containing twins, and a last third of polySi. This structure is very similar to the experimental observation schematized in Fig. 1.

IV. DISCUSSION

Using the molecular dynamics technique to simulate the annealing of an atomistic model of the FinFET, we were able to reproduce the three regions observed experimentally. The recrystallization mechanisms are not simple in this kind of structure. In order to understand the role of confinement of the core by the oxide-like shell, we simulated the annealing of the structure of Fig. 2 but without freezing some atoms to form a shell. Moreover, we applied periodic boundary conditions, also in the [010] direction. The results of the calculation on this 2D system are given in Fig. 11. In this configuration, only one grain has formed, and this grain has nucleated at the surface. In the case of the fin, two grains were formed. Even if it is not a strict demonstration, this result goes in favor of surface proximity effects on the probability of forming grains.

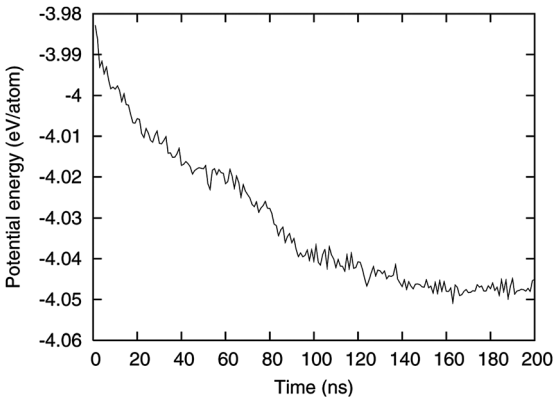

FIG. 9. Potential energy during annealing at 1700 K.

The entire height of the fin does not regrow in cSi although the annealing would have recrystallized a layer of the same height. The same conclusion was obtained experimentally for other annealing conditions (600 °C, 60s) (Ref. 5). The presence of twins and the competition of SPE with RNG prevent the regrowth in cSi. In addition, the velocity of SPE could be modified compared to bulk. We have checked that it is not the case. For this purpose, we compared the two systems after 60 ns annealing (Figs. 6 and 11), because at this stage the first twin has just formed in the fin, so the impact of this defect should not be significant. We have checked that the thickness of the recrystallized part is comparable: 58 to 64 (100)- planes for the 2D system and 58 for the fin. The presence of surfaces laterally does not reduce the velocity of SPE. These surfaces, however, are responsible for the formation of twins in the [111] direction, in agreement with the schematics of Kunii *et al.*[20]. The [111] twins were never obtained in 2D calculation on [100] oriented systems, in the

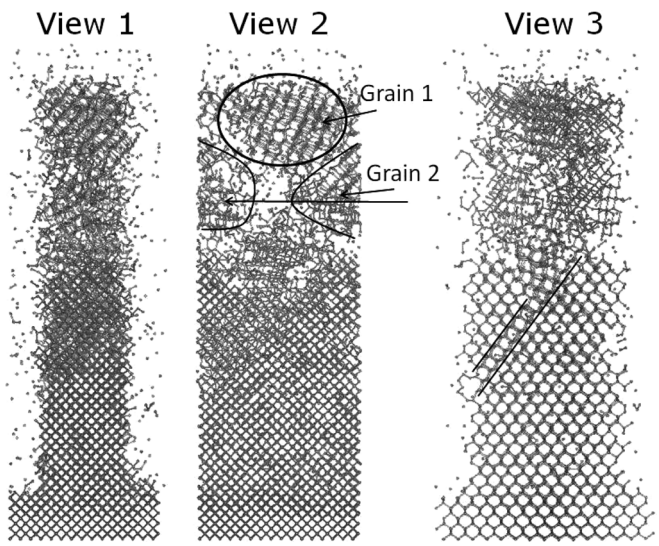

FIG. 8. Three views of the fin atomic model after 120 ns annealing. Only crystal-like atoms are represented.

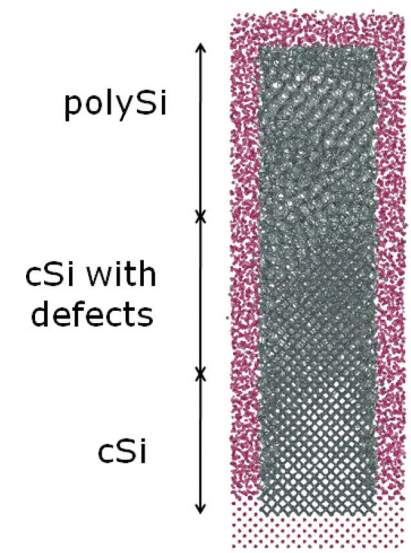

FIG. 10. (Color online) Final structure after 200 ns annealing.

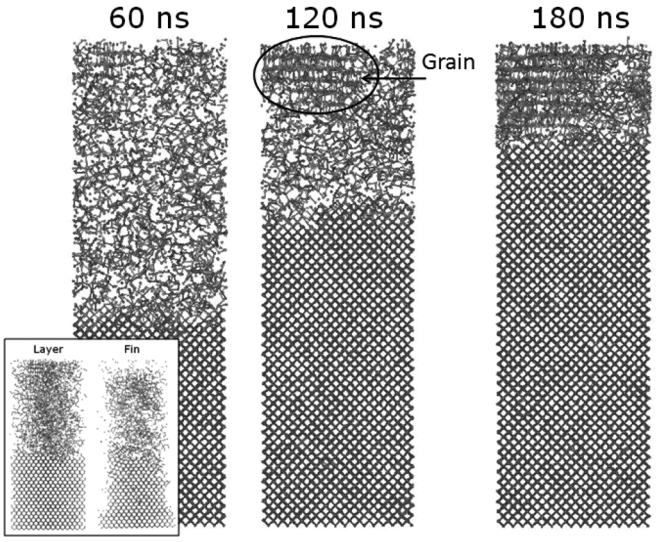

FIG. 11. Evolution of the structure without freezing atoms in the shell, and with 2D periodic boundary conditions. Inset: comparison layer/fin, 60 ns, view 2. Crystal-like atoms.

present work and in former calculations.[17] Finally, a common feature of the two systems is that the solid phase epitaxy does not absorb the grain formed by RNG: if grains form, they cannot be cured.

V. CONCLUSION

In conclusion, we performed atomistic simulations of the annealing of an amorphized silicon nanostructure using the molecular dynamics method. The atomistic model of the fin is simplified, compared to the experimental system, but retains its main features. The atomistic system after annealing is structurally similar to the experimentally observed structures, being composed of defect-free crystal, crystal with [111] twins, and polysilicon. The comparison with a 2D calculations allows one to conclude that SPE is not retarded. However, SPE is arrested when the interface of crystallization reaches the far most region where grains are formed. The influence of the surface on the probability of forming grains is also emphasized. Finally, the formation of twins is only observed in the case of the fin, which also suggests the impact of surface on their formation.

ACKNOWLEDGMENTS

The authors acknowledge Jean-Michel Droulez for the computational assistance and Professor Fabrizio Cleri for the suggestions on the manuscript. The work was part of the integrated project PULLNano funded by the European Community.

[1]G. L. Olson and J. A. Roth, Mater. Sci. Rep. **3**, 1 (1988).
[2]T. Motooka, K. Nishira, S. Munetoh, K. Moriguchi, and A. Shintani, Phys. Rev. B **61**, 8537 (2000).
[3]L. A. Marqués, L. Pelaz, M. Aboy, L. Enríquez, and J. Barbolla, Phys. Rev. Lett. **91**, 135504 (2003).
[4]A. Mattoni and L. Colombo, Phys. Rev. B **69**, 045204 (2004).
[5]R. Duffy, M. J. H. Van Dal, B. J. Pawlak, M. Kaiser, R. G. R. Weemaes, B. Degroote, E. Kunnen, and E. Altamirano, Appl. Phys. Lett. **90**, 241912 (2007).
[6]J. Tersoff, Phys. Rev. B **38**, 9902 (1988).
[7]C. Krzeminski, Q. Brulin, V. Cuny, E. Lecat, E. Lampin, and F. Cleri, J. Appl. Phys. **101**, 123506 (2007).
[8]S. Izumi, S. Hara, T. Kumagai, and S. Sakai, J. Cryst. Growth **274**, 47 (2005).
[9]M. T. Robinson and I. M. Torrens, Phys. Rev. B **9**, 5008 (1974).
[10]F. Wooten, K. Winer, and D. Weaire, Phys. Rev. Lett. **54**, 1392 (1985).
[11]W. D. Luedtke and U. Landman, Phys. Rev. B **37**, 4656 (1988).
[12]C. Krzeminski and E. Lampin, "Solid phase epitaxy amorphous silicon re-growth: some insight from empirical molecular dynamics simulation," Eur. Phys. J. B (submitted).
[13]A. Yasukawa, JSME Int. J. Ser. A **39**, 313 (1996).
[14]Y. Umeno, T. Kitamura, K. Date, M. Hayashi, and T. Iwasaki, Comput. Mater. Sci. **25**, 447 (2002).
[15]S. R. Billeter, A. Curioni, D. Fischer, and W. Andreoni, Phys. Rev. B **73**, 155329 (2006).
[16]S. Munetoh, T. Motooka, K. Moriguchi, and A. Shintani, Comp. Mater. Sci. **39**, 334 (2007).
[17]E. Lampin and C. Krzeminski, J. Appl. Phys. **106**, 063519 (2009).
[18]S. Nosé, Mol. Phys. **52**, 255 (1984).
[19]W. G. Hoover, Phys. Rev. A **31**, 1695 (1985).
[20]Y. Kunii, M. Tabe, and K. Kajiyama, J. Appl. Phys. **56**, 279 (1984).